applied sciences

MDPI

Article

Three-Dimensional Kinematics and Kinetics of the Overhead Deep Squat in Healthy Adults: A Descriptive Study

Barbara J. Hoogenboom *, Christopher J. May, Gordon J. Alderink, Brian S. Thompson and Lukas A. Gilmore

Department of Physical Therapy and Athletic Training, Grand Valley State University, Grand Rapids, MI 49503, USA; maych@mail.gvsu.edu (C.J.M.); aldering@gvsu.edu (G.J.A.); thompsbs@mail.gvsu.edu (B.S.T.); gilmorlu@mail.gvsu.edu (L.A.G.)
* Correspondence: hoogenbb@gvsu.edu; Tel.: +1-616-331-2695

Abstract: The squat, a fundamental functional movement, is prone to biomechanical inefficiencies. Several screening batteries utilize the Overhead Deep Squat (OHDS) to assess individuals for stability and mobility deficits. The purpose of this study was to create a comprehensive description of the three-dimensional (3D) kinematics and kinetics for normal, healthy participants during an overhead deep squat. This descriptive study containing 70 healthy young adults (31 male, 39 female; aged 18–35) utilized a video motion tracking system interfaced with force plates to obtain full-body 3D kinematics and kinetics. Seventy-three retro-reflective markers from the combined Plug-in Gait, Vicon upper limb, and Oxford Multi-segment foot models were used. Visual 3D software was used to determine joint kinematics and kinetics. Means and standard deviations of lower limb and trunk segment joint angles in the sagittal, transverse, and horizontal planes, as well as the ground reaction forces and net internal joint moments, were computed. The largest movements and joint moments occurred in the sagittal plane; however, the frontal and transverse plane appear crucial to providing stability and mobility. These results can be used as pilot normative data for both future studies and during assessments of biomechanical abnormalities in training and rehabilitation settings.

Keywords: functional movement; kinematics; kinetics; overhead deep squat

check for updates

Citation: Hoogenboom, B.J.; May, C.J.; Alderink, G.J.; Thompson, B.S.; Gilmore, L.A. Three-Dimensional Kinematics and Kinetics of the Overhead Deep Squat in Healthy Adults: A Descriptive Study. *Appl. Sci.* **2023**, *13*, 7285. https://doi.org/10.3390/app13127285

Academic Editors: Weijie Wang and Dong Ming

Received: 10 May 2023
Revised: 3 June 2023
Accepted: 5 June 2023
Published: 19 June 2023

Copyright: © 2023 by the authors. Licensee MDPI, Basel, Switzerland. This article is an open access article distributed under the terms and conditions of the Creative Commons Attribution (CC BY) license (https://creativecommons.org/licenses/by/4.0/).

1. Introduction

The squat is a fundamental human movement incorporated into many daily activities and is used by all ages and functional levels. The Overhead Deep Squat (OHDS), a variation of the deep squat with placement of the upper extremities at an end-range ulno-humeral extension and glenohumeral elevation, is a multi-segment movement that requires trunk control, the sequencing of muscular actions, and an available range of motion (ROM) at multiple joints to perform efficiently [1]. Clinical assessment of the OHDS takes place frequently as a part of the Functional Movement Screen™ (FMS™), a test battery performed to assess the mobility and stability of individuals in populations, such as, but not limited to, active adults and youth, collegiate athletes, and military service members [2–5].

The OHDS is one of seven fundamental movements in the FMS™ that has been used to screen motor performance and predict performance on the FMS™ [6]. Conflicting evidence exists on the predictive validity of the FMS™ regarding injuries [2,3,7,8]. Despite this, multiple authors have found good-to-excellent intra-rater reliabilities for rating performance of the components of the FMS™ (ICC = 0.87–0.90) among both novice and expert testers with pooled interrater reliability among both novice and experts of 0.81 [8,9].

Since the OHDS is considered a closed kinetic chain activity, the subtalar and talocrural joints are critical to the proper movement and positioning of proximal segments [10]. It has been shown that the degree of talocrural dorsiflexion during squatting movements alters knee frontal and sagittal plane kinetics and kinematics, as well as lumbar and thoracic spine kinematics [10–13]. Unfortunately, the models used by these studies failed to capture

the relationship between the segments of the foot, which may omit information critical to the proper understanding of the OHDS throughout the kinetic chain.

Three-dimensional (3D) motion capture allows for the accurate assessment of complex dynamic human movement patterns and has been used to accurately measure kinetics and kinematics in various types of squat forms [10,11,14–17]. The authors were unable to find research using 3D motion capture technology detailing forefoot positioning during squatting. However, in a 3D motion capture study of the knee and hip, individuals with forefoot varus demonstrated increased hip internal rotation during a single leg squat (SLS) [18]. Another study by Butler et al., in which only sagittal plane data were analyzed, found that those who scored better on the OHDS component tended to utilize greater ankle dorsiflexion excursion, peak knee flexion, knee flexion excursion, knee extension moment, peak hip flexion, hip flexion excursion, and hip extension moment when compared to lesser scoring groups [10]. Researchers have also examined gender differences in squat kinematics and kinetics, finding that males display greater peak knee valgus and hip flexion angles, as well as vertical ground reaction forces and peak hip extension moments, while also demonstrating reduced ankle dorsiflexion and hip rotation excursion [19,20]. Finally, Heredia et al. found that those who better performed the OHDS, as scored by the FMS™, demonstrated statistically greater hip flexion, knee flexion, knee internal rotation, and ankle dorsiflexion angles compared to those who scored less well [15].

A descriptive dataset including the foot and ankle, which would provide raters with more detailed information in their assessment of the movement pattern, does not exist in the literature [11,12,16,21,22]. Due to the lack of a normalized comparative dataset that includes more detailed kinematic data on foot movement, evaluation of patients' OHDS compensations is often difficult for clinicians, beyond the dichotomous score. Three-dimensional motion capture and analysis allow for a detailed description and evaluation of the motion, internal joint moments, and ground reaction forces acting on the human body, enabling the creation of such a dataset.

Kinematic variables can be observed during the OHDS at the shoulder, trunk, pelvis, hip, knee, ankle, foot, and hallux joint/segment angles in the frontal, sagittal, and transverse planes, yet detailed movements in the foot are subtle in the frontal and transverse planes and not detectable observationally. The kinetic variables during the OHDS include ground reaction forces (GRF), as well as net internal joint moments and powers at the hip, knee, and ankle. The existing literature does not include a detailed 3D analysis of the foot throughout the OHDS. Therefore, the purpose of this study was to create a comprehensive description of the 3D kinematics and kinetics for normal, healthy participants during an OHDS.

2. Materials and Methods

2.1. Study Design

The data for this descriptive study were captured in single sessions in a biomechanics laboratory over the span of three years.

2.2. Informed Consent

This research was approved by the Grand Valley State University Institutional Review Board (14-026-H). All participants completed informed consent documentation on the day of testing.

2.3. Participants

A sample of convenience of self-reported healthy, active participants between the ages of 18 and 35 years was recruited. Exclusion criteria included the following: any past history of orthopedic surgical intervention to the extremities and/or vertebral column, musculoskeletal orthopedic injury within the prior six months, somatosensory disorders that affected balance, or a score of zero (indicating pain during movement) on any subtest based on the Functional Movement Scale (FMS™). Injury histories were recorded and evaluated as part of inclusion/exclusion screening, and all included subjects were deemed

appropriate to participate based on prior injury history. All subjects were assessed using the FMS™ (conducted and scored using previously published methods [23]) to assure pain-free performance of fundamental movements, including the OHDS. Participants were screened for foot type and rear-, mid-, and forefoot position, which was used during marker placement in the Oxford foot model (OFM).

2.4. Instrumentation

The Vicon Motion Lab Systems 600 series and 8 MX-T40 cameras (Oxford Metrics, Oxford, UK) and Nexus motion capture software (Vicon Motion Systems Ltd., Oxford, UK) were used to record (120 Hz) marker trajectories. Two floor-embedded force plates (Advanced Mechanical Technology Inc., Watertown, MA, USA) were utilized to record GRFs, moments, and centers of pressure. Force data were collected at 1200 Hz with one plate located beneath each foot for the collection of GRFs. Trajectory data were filtered using Woltring (MSE 15), and raw force data were filtered using a zero-lag 4th order Butterworth (cut-off 6 Hz) [24,25].

Procedures

Anthropometric measures included the following: height and body mass, as well as measures needed for the Plug-in-Gait (PIG) model (leg length, pelvic width, ankle and knee width, shoulder offset, elbow width, wrist width, and hand thickness). Retroreflective markers were placed directly on the skin using hypoallergenic double-sided tape according to the PIG model, OFM, and Vicon upper limb models [10,17,26–31]. The PIG model was modified by the placement of medial knee and ankle markers. Nine-millimeter (mm)-diameter markers were placed on the feet. Foot markers were placed with the participants in a standing position in their preferred foot position, i.e., neutral, planus, or cavus. Medial and lateral hindfoot and midfoot markers were placed to best represent that position. Fourteen-millimeter markers were used at the other anatomical locations. To control for inter-rater variability within a study and between studies over three years, one trained researcher placed all markers. To ensure the fidelity of consistent and accurate marker placement three procedures were followed: (1) only one researcher for any given study year placed all markers; (2) marker placement was immediately checked by the senior researcher; (3) prior to experimental data collection, pilot gait data were collected and kinematic data were reduced and graphed relative to the laboratory control data set. Novice researchers were required to demonstrate lower extremity joint angle graphics to be within one standard deviation of the laboratory control data set (created by the lab director).

Prior to squat data collection, a static subject calibration trial was performed and processed to create a unique subject skeletal model. The subjects were instructed to stand in the middle of the calibrated volume in an anatomical position with feet shoulder-width apart, knees slightly bent, and arms slightly abducted for four seconds. In addition, one walking trial was collected and processed, and kinematic data were graphed to assess the accuracy of marker placement on lateral and medial femoral condyles and thigh and tibial segments [32]. If hip internal/external rotation or knee varus/valgus joint angles exceeded the pre-determined normal band of one standard deviation outside the control mean, lateral thigh, medial femoral condyle, and lateral tibial marker placements were corrected, and the static subject calibration was repeated. A second gait trial would be checked for corrected hip and knee joint angles.

After the accuracy of markers and related hip and knee kinematics were verified, OHDS data were captured. Participants were instructed by an examiner to complete the OHDS according to standard FMS™ instructions. These instructions were standardized to the FMS™ protocol for generalizability and applicability to assessment tools used in clinical settings. The motion capture procedure occurred as follows.

Motion capture was initiated when the subjects were standing behind the force plates with hands down holding a dowel. Participants stepped forward onto the force plates with one foot placed in the center of each force plate, feet shoulder-width apart, toes

pointing generally forward (a standard foot position for all participants was not dictated) as comfortable for the subject without allowing greater than 15° talocrural rotation. The squat was performed to the subject's self-selected maximum depth with the dowel above their heads before returning to the starting position and stepping back off the force plates (Figure 1). Participants repeated the OHDS three times stepping off the force plate and stopping motion capture between each trial. If directions were not followed correctly, an additional trial was performed.

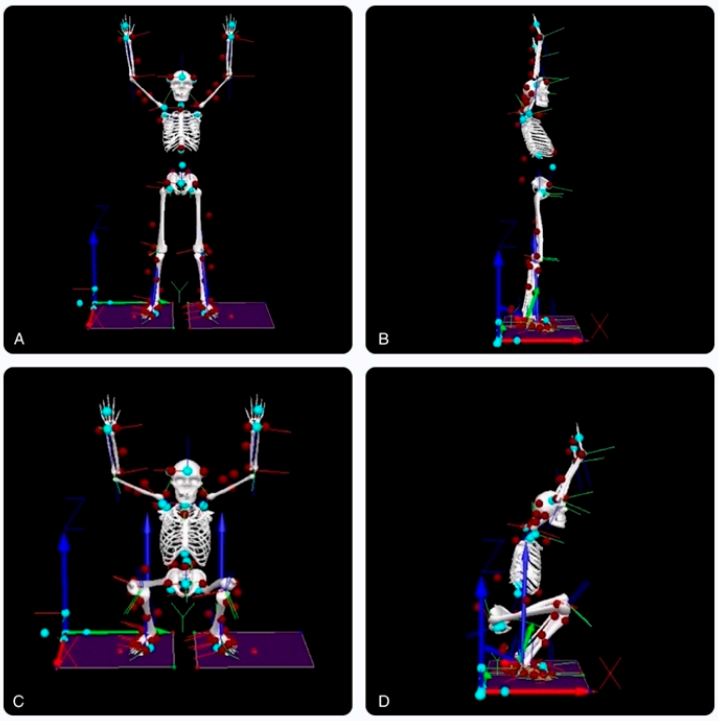


Figure 1. Example data collection set up for 3-D motion capture of the OHDS. (**A**) Beginning position, sagittal view; (**B**) beginning position frontal view; (**C**) 50% (full squat position) sagittal view; (**D**) 50% (full squat position) frontal view. The two blue arrows projecting upward represent the vertical ground reaction forces. The three arrows on the corner of the force plates represent the plate coordinate system: x (red), y (green), and z (blue).

2.5. Data Reduction and Analysis

Raw data were processed using Nexus software. After reconstruction and labeling/relabeling, gaps in the trajectories were filled using a combination of the following Nexus editing routines: spline, pattern fill, and rigid-body fill. Trajectory and raw ground reaction force data were filtered using Nexus pipelines. Additional Nexus pipelines were also implemented to create events to define the squat cycle. Based on an observation, the initiation of the squat was marked when the posterior superior iliac spine (PSIS) marker on the pelvis began to move, the endpoint of the squat was marked at the most inferior position of the PSIS marker, and return-to-neutral was marked when the PSIS marker reached its most superior position. Thus, the initiation to the endpoint defined the descent phase (0–50%), and the endpoint to return defined the ascent phase of the squat (51–100%).

Three representative squat trials from each participant were exported to Visual3D (C-Motion, Germantown, MD, USA) for further dynamic processing and statistical descriptive analysis, i.e., determination of mean and standard deviation kinematic and kinetic curves. Joint angles were calculated using a Cardan rotation sequence, i.e., x-y-z. The biomechanical model created in Visual3D used the Harrington method for estimating hip joint center location [28,30,33]. Pelvic and trunk segmental motion was determined using the Euler sequence z-y-x [34]. Oxford foot model multi-segment foot angles were determined using the following rotation sequences: tibia/forefoot x-y-z; tibia/hindfoot and

hindfoot/forefoot x-z-y; and forefoot/hallux x-y-z [27]. Visual 3D was also used to determine GRFs, and net internal hip, knee, and ankle joint moments (Nm.kg), and sagittal plane powers (W/kg), normalized to body mass. Normal mean (± standard deviation) kinematic and kinetic data figures were created in the most current Visual 3D (Vx64) software and graphed as the percent squat from 0 to 100%. This is consistent with time-normalized reporting of the OHDS used by Heredia et al. where graphic presentation is reported in a percentage from 0 to 100% [15].

3. Results

3.1. Sample Demographics

Seventy-two healthy subjects aged 20–33 years (32 male and 40 female) participated (Table 1). For the analysis of data for this project, we did not separate results by gender. Data from two subjects were unable to be processed and were not included in analyses (one male, one female).

Table 1. Participant characteristics.

Characteristic			
Sex	**Male (N = 32)**	**Female (N = 40)**	**All (N = 72)**
Age (y)	24.93 ± 2.7	23.55 ± 2.7	24.16 ± 2.8
Height (cm)	180.1 ± 7.3	165.5 ± 6.3	171.3 ± 10.3
Weight (kg)	80.9 ± 10.3	58.9 ± 7.8	68.5 ± 14.1
BMI (kg/m^2)	25.0 ± 4.1	21.8 ± 2.4	23.2 ± 3.6

Descriptive Kinematic and Kinetic Results

Table 2 provides the results of the kinematic and kinetic analyses for each phase of the OHDS. These data were used to prepare graphic representations of each segment of the body during the motion.

Table 2. Overhead deep squat kinematic and kinetic data reported by percentage of squat completion (1, 25, 50, 76, and 100%) for all subjects, for the left lower extremity, presented as mean (SD).

	1%	**25%**	**50%**	**76%**	**100%**
Kinematics (All Reported in Degrees)					
L HF/FF Dorsi/Plantarflexion	−1.59 (4.17)	7.70 (5.18)	10.82 (5.41)	7.86 (5.37)	−2.38 (3.92)
L HF/FF Add/Abduction	6.35 (4.89)	7.32 (4.86)	6.99 (4.94)	6.79 (4.67)	6.16 (4.87)
L HF/FF Sup/Pronatio	−5.34 (6.23)	−6.07 (6.48)	−6.86 (6.65)	−5.98 (6.58)	−5.13 (6.31)
Tibia/FF Dorsi/Plantarflexion	0.89 (4.09)	22.78 (6.65)	30.31 (5.83)	22.40 (8.02)	−1.29 (3.62)
L Tibia/FF Add/Abduction	8.06 (4.35)	8.64 (6.45)	3.30 (7.06)	6.90 (6.19)	7.25 (4.30)
L Tibia/FF Sup/Pronation	4.17 (8.88)	1.54 (9.33)	−2.57 (9.65)	0.51 (9.48)	3.71 (8.83)
L Tibia/HF Dorsi/Plantarflexio	3.44 (3.48)	15.76 (5.99)	19.28 (5.90)	14.92 (6.41)	1.82 (3.59)
L Tibia/HF Add/Abduction	1.96 (3.71)	0.32 (4.78)	−4.42 (5.06)	−0.56 (4.73)	1.44 (3.98)
L Tibia/HF Sup/Pronation	9.38 (6.11)	7.59 (6.20)	3.47 (6.38)	6.65 (6.07)	8.69 (5.83)
L TFJ Flexion/Extension	0.22 (6.43)	68.29 (14.91)	122.88 (17.47)	78.20 (21.29)	−1.14 (5.85)
L TFJ Varus/Valgus	0.04 (2.55)	0.72 (7.18)	0.28 (9.66)	−1.25 (8.52)	0.10 (2.68)
L TFJ Rotation	−17.66 (8.90)	−6.01 (8.61)	3.45 (11.67)	−5.50 (8.83)	−15.75 (9.16)
L Hip Flexion/Extension	10.50 (6.03)	75.24 (13.92)	118.74 (13.22)	84.47 (16.71)	12.77 (7.36)
L Hip Add/Abduction	−0.81 (2.83)	−16.00 (5.17)	−19.33 (5.55)	−15.15 (5.57)	−7.95 (2.75)
L Hip Rotation	−4.33 (8.40)	−4.24 (9.22)	10.65 (14.09)	−2.97 (11.72)	−7.08 (7.98)
L Pelvic Anterior Tilt	15.27 (4.61)	32.86 (6.86)	26.90 (11.55)	31.00 (6.92)	16.47 (5.55)

Table 2. *Cont.*

	1%	25%	50%	76%	100%
Kinematics (All Reported in Degrees)					
L Pelvic Obliquity	0.56 (1.39)	1.16 (1.96)	1.14 (2.82)	0.87 (2.12)	0.50 (1.47)
L Pelvic Rotation	−0.87 (2.35)	−0.74 (2.02)	−0.14 (2.17)	0.16 (2.45)	−0.63 (2.09)
L Trunk Rel to Pelvis Forw/Backw lean	24.16 (5.88)	21.04 (6.65)	−5.06 (13.91)	9.56 (10.35)	21.47 (6.07)
L Trunk Rel to Pelvis Lateral Lean	0.58 (1.69)	0.87 (1.91)	0.93 (2.70)	0.77 (2.23)	0.54 (1.95)
L Trunk Rel to Pelvis Rotation	−0.10 (3.59)	0.12 (3.21)	0.17 (3.17)	0.10 (3.11)	−0.08 (3.35)
L Trunk Forw/Backw Lean	8.90 (3.06)	−11.80 (5.98)	−31.91 (10.13)	−21.41 (8.72)	4.99 (3.88)
L Trunk Lateral Lean	0.05 (1.10)	−0.33 (1.46)	−0.25 (2.13)	−0.12 (1.98)	0.08 (1.23)
Left Trunk Rotation	−0.88 (2.93)	−0.84 (2.77)	−0.48 (2.52)	−0.10 (2.80)	−0.64 (2.81)
L Shoulder Abduction	126.61 (8.18)	126.29 (8.99)	125.49 (9.47)	125.00 (9.35)	121.81 (10.31)
L Shoulder External Rotation	80.92 (16.31)	82.14 (17.01)	83.93 (17.83)	81.45 (17.42)	77.50 (16.31)
Kinetics					
L Ankle Plantar/Dorsi Moment (Nm/kg)	0.28 (0.01)	0.16 (0.11)	0.23(0.16)	0.11(0.08)	0.25(0.10)
L Ankle Ev/Inv Moment (Nm/kg)	0.03 (0.05)	−0.03 (0.05)	−0.09 (0.06)	−0.03 (0.05)	0.03 (0.04)
L Ankle Ext/Int Moment (Nm/kg)	0.03 (0.03)	0.05 (0.04)	0.05 (0.05)	0.04 (0.04)	0.03 (0.03)
L Ankle Power (Watts/kg)	−0.01 (0.02)	−0.06 (0.06)	0.00 (0.02)	0.05 (0.05)	0.00 (0.07)
L TFJ Flex/Ext Moment (Nm/kg)	−0.14 (0.13)	0.62 (0.21)	0.80 (0.25)	0.68 (0.22)	−0.18 (0.12)
L TFJ Valgus/Varus Moment (Nm/kg)	−0.03 (0.06)	0.05 (0.11)	0.27 (0.21)	0.04 (0.15)	−0.03 (0.07)
L TFJ Ext/Int Moment (Nm/kg)	0.03 (0.03)	0.08 (0.08)	0.30 (0.12)	0.08 (0.06)	0.02 (0.03)
L TFJ Power (Watts/kg)	0.02 (0.04)	−1.09 (0.50)	−0.27 (0.35)	1.37 (0.51)	0.00 (0.03)
L Hip Flex/Ext Moment (Nm/kg)	0.00 (0.13)	0.43 (0.19)	0.77 (0.20)	0.57 (0.22)	0.05 (0.14)
L Hip Add/Abduction Moment (Nm/kg)	0.01 (0.07)	−0.18 (0.13)	−0.54 (0.16)	−0.21 (0.20)	0.00 (0.08)
L Hip Ext/Int Moment (Nm/kg)	0.03 (0.03)	0.07 (0.09)	−0.14 (0.15)	0.05 (0.11)	0.03 (0.05)
L Hip Power (Watts/kg)	0.00 (0.02)	−0.40 (0.19)	−0.13 (0.17)	0.52 (0.20)	0.01 (0.03)
Left Vertical GRF (% body weight)	0.51 (0.04)	0.48 (0.05)	0.55 (0.07)	0.50 (0.05)	0.51 (0.05)
Left Posterior/Anterior GRF (% body weight)	0.07 (0.01)	0.05 (0.02)	−0.01 (0.04)	0.05 (0.26)	0.07 (0.02)

L: left, HF: hindfoot, FF: forefoot, TFJ: tibiofemoral Joint, Rel: relative, forw/backw: forward/backward, GRF: ground reaction forces, Plantar/Dorsi: plantar/dorsiflexion, Ev/Inv: eversion/inversion, Ext/Int: external/internal rotation, Flex/Ext: flexion/extension.

3.2. Forefoot, Hindfoot, and Tibia Kinematics

3.2.1. Forefoot Relative to Hindfoot (HF/FF)

The mean range of motion during the squat ran from approximately 2° plantar flexion to 10° dorsiflexion, with a mean peak HF/FF dorsiflexion of 10.82° ± 5.41 at 50% of the squat. The HF/FF maintained approximately 5–7° abduction and 6–7° supination throughout the squat (Figure 2).

3.2.2. Forefoot (FF) Relative to Tibia

The mean range of motion spanned from approximately 0° to 30° of dorsiflexion, with a mean peak tibia/FF dorsiflexion of 30.31° ± 5.83° at 50% of the squat. The mean motion of the tibia/FF ran from approximately 4° of adduction to 2° of abduction before returning to an adducted position, while the mean tibia/FF supination ranged from approximately 3° to 8° (Figure 3).

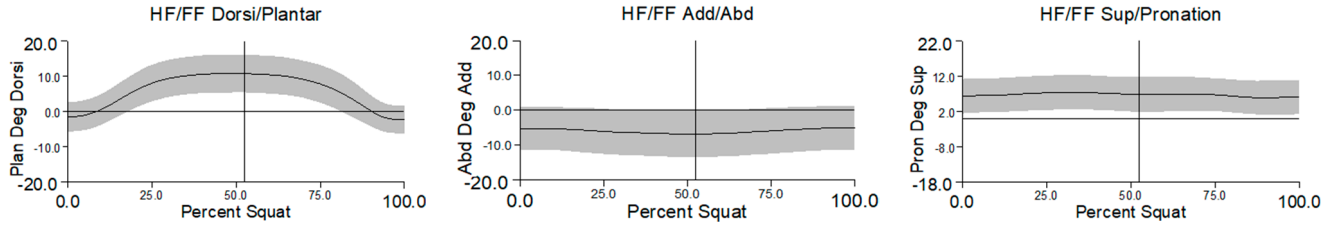


Figure 2. Mean (±SD) forefoot (FF) relative to hindfoot (HF) joint angles. The dark line represents the sample mean and the gray band surrounding the mean value represents +/− one standard deviation.

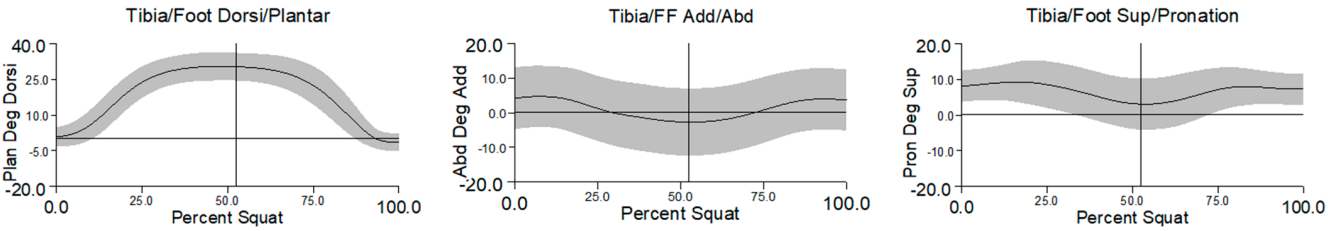


Figure 3. Mean (±SD) tibia relative to forefoot joint angles. The dark line represents the sample mean and the gray band surrounding the mean value represents +/− one standard deviation.

3.2.3. Hindfoot (HF) Relative to Tibia

The mean tibia/HF dorsiflexion approximated 0° to 20°, with a mean peak dorsiflexion of 19.28° ± 5.90° at 50% of the squat. With squat initiation, the hindfoot was inverted approximately 2°, everted to about 4°, and then returned to an inverted position during ascent. The hindfoot was internally rotated throughout the squat, cycling from 9° to 3° at mid-squat then back to 9° at the completion of the squat (Figure 4).

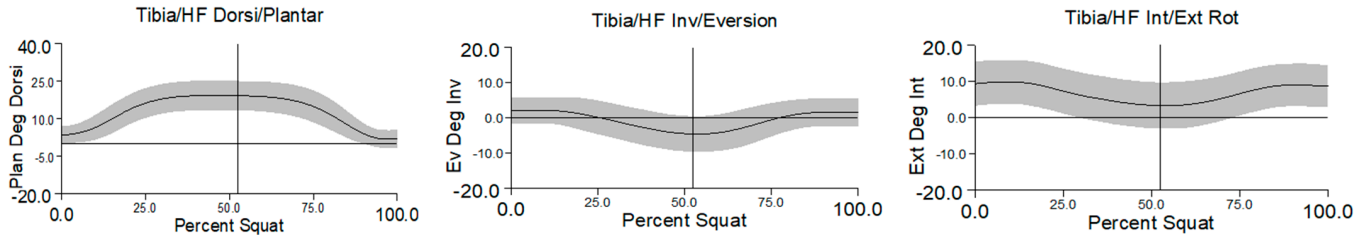


Figure 4. Mean (±SD) tibia relative to hindfoot joint angles (degrees). The dark line represents the sample mean and the gray band surrounding the mean value represents +/− one standard deviation.

3.3. Kinetics—Ankle Joint Moments and Power

The mean net ankle plantarflexor moments ranged from approximately 0.3 Nm/k at 0% to 0.1 Nm/kg at 75% of the squat. Frontal and transverse plane ankle internal moments were very small (Figure 5).

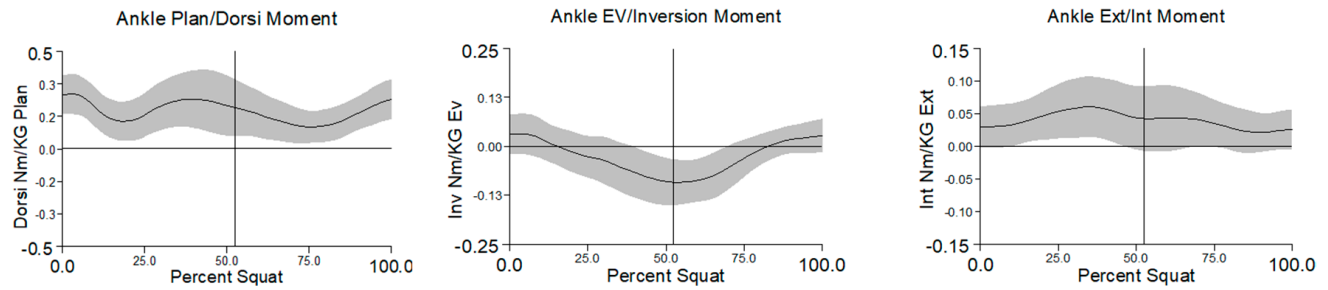


Figure 5. Mean (±SD) joint moments of the ankle (Nm/kg). The dark line represents the sample mean and the gray band surrounding the mean value represents +/− one standard deviation.

The mean ankle power ranged from approximately 0.10 W/kg absorption on squat descent to 0.10 W/kg generation on the ascent (Figure 6).

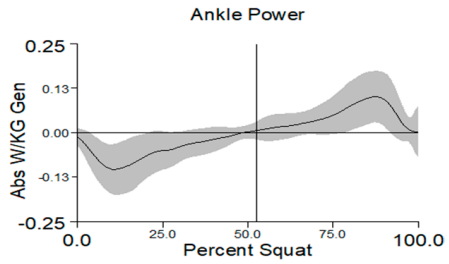


Figure 6. Mean (±SD) ankle power (watts/kg). The dark line represents the sample mean and the gray band surrounding the mean value represents +/− one standard deviation.

3.4. Tibiofemoral Joint (TFJ) Kinematics

The mean range of motion spanned from approximately 0° to 123° of the TFJ flexion during the squat. The mean TFJ varus/valgus mobility was negligible throughout the squat; however, variability was large. Knee axial rotation cycled from approximately 16° of external rotation to 3° internal rotation and back to external rotation (Figure 7).

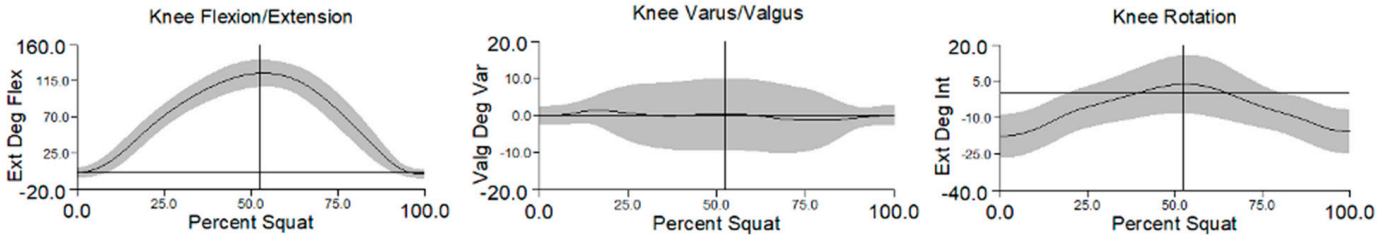


Figure 7. Mean (±SD) femur on tibia joint angles (Degrees). The dark line represents the sample mean and the gray band surrounding the mean value represents +/− one standard deviation.

3.5. Kinetics—TFJ Moments and Power

The TFJ begins and ends with a net mean flexor moment of approximately 0.16 Nm/Kg and had a mean peak extensor moment of approximately 0.85 Nm/kg. In the frontal plane, despite negligible movement, the mean range of TFJ moments ran from a net varus moment of 0.03 Nm/kg to a net valgus moment of 0.27 Nm/kg. The mean knee external rotator moments ranged from approximately 0.03 Nm/kg to 0.30 Nm/kg (Figure 8).

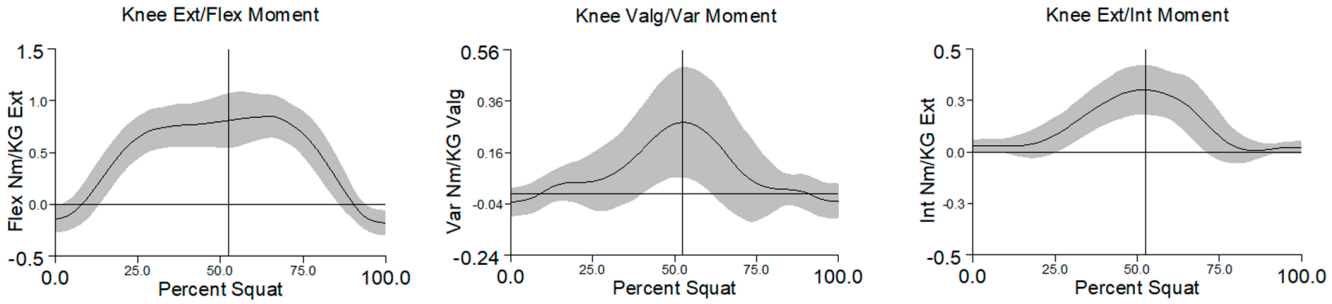


Figure 8. Mean (±SD) femur on tibia joint moments (Nm/kg). The dark line represents the sample mean and the gray band surrounding the mean value represents +/− one standard deviation.

The mean tibiofemoral joint power ranged from approximately 1.1 W/kg absorption on squat descent to 1.1 W/kg generation on the ascent (Figure 9).

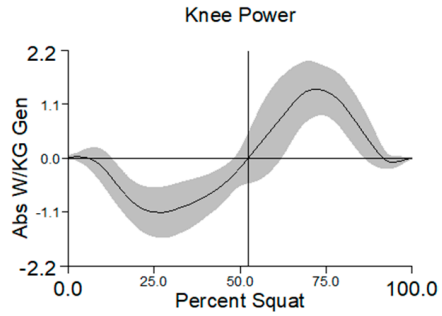


Figure 9. Mean (±SD) knee power (watts/kg). The dark line represents the sample mean and the gray band surrounding the mean value represents +/− one standard deviation.

3.6. Hip Joint Kinematics

The mean range of motion of the hip flexion during the squat spanned from approximately 11° to 119° before returning to 13°. Mean hip adduction ranged from approximately 8° to 19° throughout the squat. Initially, the hip started in approximately 4° of external rotation and then achieved 11° of internal rotation before returning to 8° of external rotation (Figure 10).

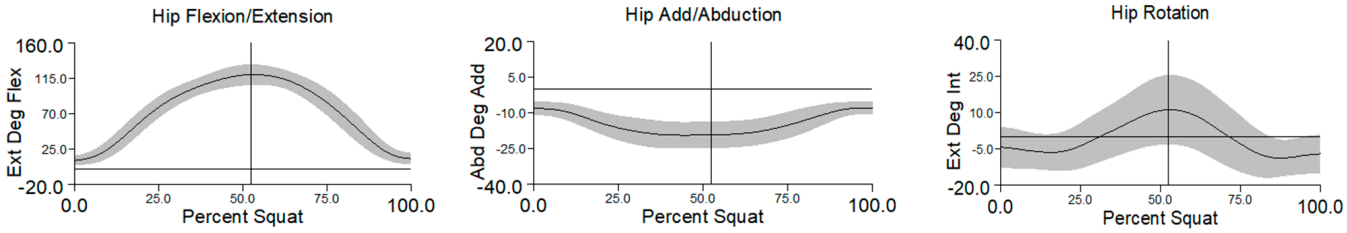


Figure 10. Mean (±SD) hip joint angles (degrees). The dark line represents the sample mean and the gray band surrounding the mean value represents +/− one standard deviation.

3.7. Kinetics—Hip Joint Moments and Power

The mean range of net hip joint extensor moments ran from approximately 0 Nm/kg to 0.8 Nm/kg with a mean peak moment of 0.77 ± 0.20 at 50% of the squat. Hip abductor moments approximated 0 Nm/kg at the beginning and end of the squat, with a peak mean hip adductor moment of approximately 0.5 Nm/kg. The mean range of hip joint moments ran from a hip external rotator moment of approximately 0.09 Nm/kg to an internal rotator moment of 0.14 Nm/kg (Figure 11).

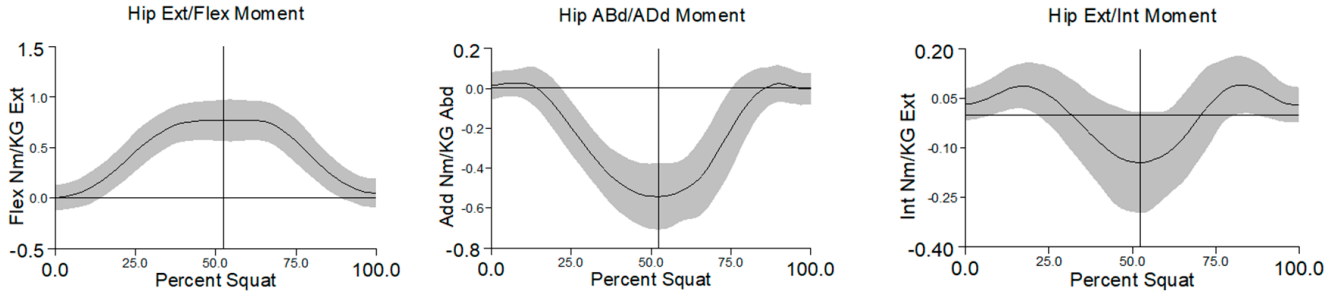


Figure 11. Mean (±SD) hip joint moments (Nm/kg). The dark line represents the sample mean and the gray band surrounding the mean value represents +/− one standard deviation.

The mean range of hip power spanned from approximately 0.4 W/kg power absorption to approximately 0.5 W/kg power generation (Figure 12).

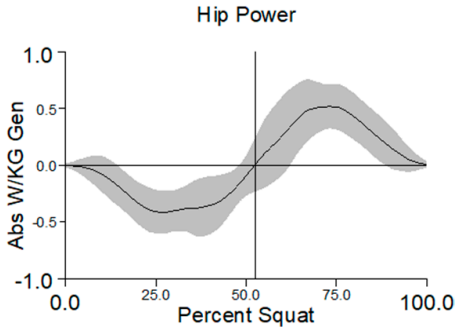


Figure 12. Mean (±SD) hip joint power (Watts/kg). The dark line represents the sample mean and the gray band surrounding the mean value represents +/− one standard deviation.

3.8. Pelvic Kinematics

The mean range of motion oscillated between approximately 15° and 33° of the anterior pelvic tilt throughout the squat. The mean pelvic obliquity and rotation were negligible throughout the squat (Figure 13).

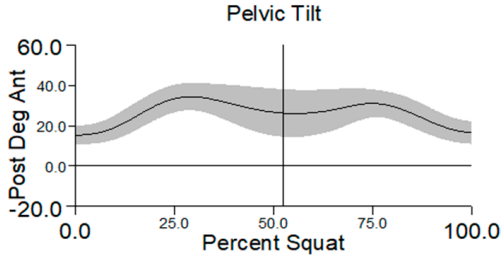


Figure 13. Mean (±SD) pelvic tilt (degrees). The dark line represents the sample mean and the gray band surrounding the mean value represents +/− one standard deviation.

3.8.1. Trunk Motion Relative to the Pelvis

The mean range of motion of the trunk relative to the pelvis spanned from approximately 24° of forward lean to 5° of backward lean before returning to 21° of forward lean at the end of the squat. The mean trunk lateral lean and rotation relative to the pelvis were negligible throughout the squat (Figure 14).

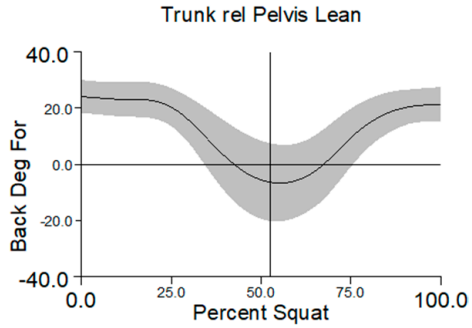


Figure 14. Mean (±SD) trunk relative to pelvis lean (degrees). The dark line represents the sample mean and the gray band surrounding the mean value represents +/− one standard deviation.

3.8.2. Trunk Motion Relative to Laboratory Coordinate System

The mean range of motion during the squat spanned from approximately 9° of the forward trunk lean to 32° of the backward lean before returning to 5° of the forward lean. The mean trunk lateral lean and rotation were negligible throughout the squat (Figure 15).

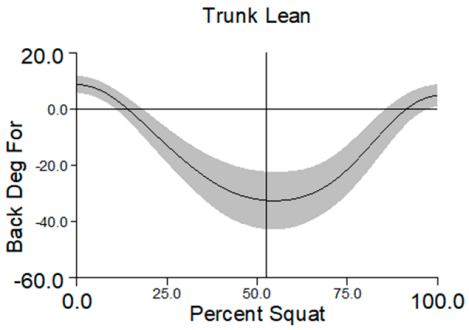


Figure 15. Mean (±SD) trunk lean (degrees). The dark line represents the sample mean and the gray band surrounding the mean value represents +/− one standard deviation.

3.9. Upper Extremity Kinematics (Humerus Relative to the Trunk Segment)

The mean range of shoulder abduction was between 120° and 130° throughout the squat. The mean range of shoulder external rotation was between 75° and 85° throughout the squat. Both shoulder abduction and external rotation had considerable variation (Figure 16).

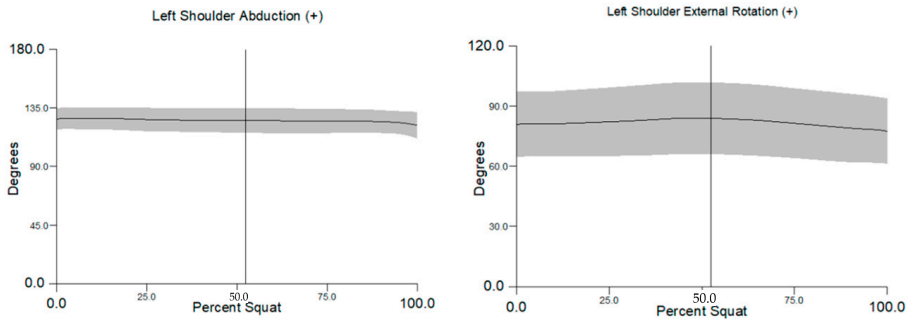


Figure 16. Mean (±SD) left shoulder joint angle (degrees). The dark line represents the sample mean and the gray band surrounding the mean value represents +/− one standard deviation.

3.10. Ground Reaction Forces (GRFs)

The mean vertical GRF ranged from 45% and 60% BW (Figure 17) per leg throughout the squat. The mean GRF in the anterior–posterior component was less than 10% BW per leg throughout the squat (Figure 18).

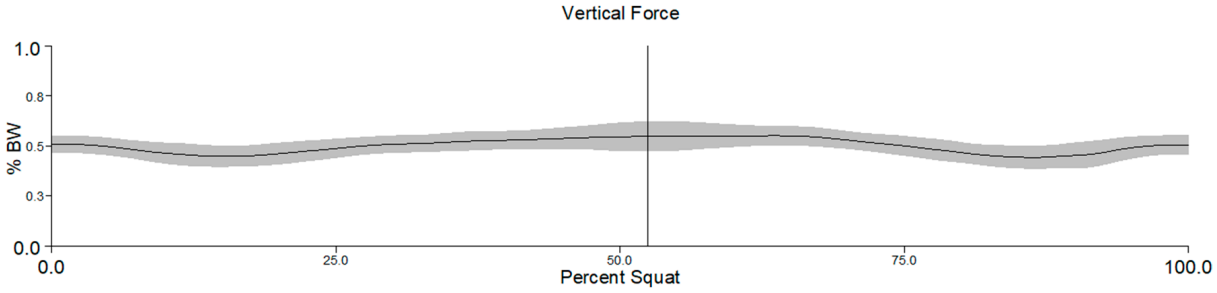


Figure 17. Mean (±SD) vertical ground reaction forces (percentage of body weight). The dark line represents the sample mean and the gray band surrounding the mean value represents +/− one standard deviation.

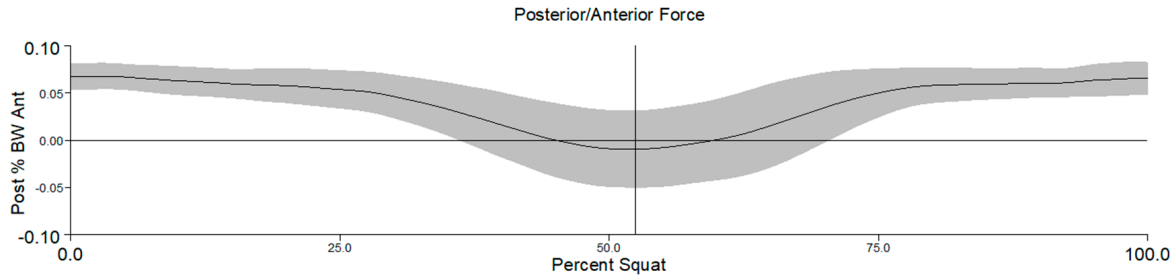


Figure 18. Mean (±SD) posterior/anterior ground reaction forces (percentage of body weight). The dark line represents the sample mean and the gray band surrounding the mean value represents +/− one standard deviation.

The mean GRF in the medial-lateral component was negligible.

4. Discussion

There are a number of tests used to identify abnormal movement patterns that may contribute to injury risk in athletes. The FMS^{TM}, an aggregate of seven tests, was developed to identify movement asymmetry and/or dysfunctional movement patterns of the trunk, pelvis, and upper and lower extremities [10,23]. As a component of the FMS^{TM}, the OHDS is a performance-oriented test of mobility and stability of multiple joints and appears to contribute the largest proportion of variance to the composite FMS^{TM} score [10,15]. Despite the obvious need for multiplanar controlled mobility for the completion of a full, pain-free deep squat, there exists no comprehensive control dataset of the 3D joint movement elements of the OHDS. Furthermore, previous biomechanical models used to examine the OHDS have not included the means to assess the 3D movements of the foot. Therefore, the purpose of this study was to assess the 3D kinematics and kinetics of the entire lower extremity and shoulder associated with the OHDS.

Although participants for this project were screened using the entire FMS^{TM}, they were not distinguished by score. However, those who scored a zero were excluded from participation. In general, our results demonstrated that sagittal plane movements at the hip, knee, and ankle were comparable to what had previously been reported. Internal net plantar flexor and extensor moments were dominant at the ankle, knee, and hip, respectively, at a full squat. Sagittal plane movements dominated the mobility of the trunk and pelvic segments, with a pattern of backward trunk lean and anterior pelvic tilt at a full squat. Healthy, young individuals were able to maintain shoulder abduction/external rotation during the entire squat. Similar to what has been reported for the stance phases of walking and running, in order to keep the foot flat during a full squat there was coupled motion at the hip, knee, and ankle/foot [35–37]. As participants descended, the hip and knee joints internally rotated as the ankle reached the maximum dorsiflexion, and the hindfoot (i.e., tibia/HF) everted and the forefoot (HF/FF and tibia/foot) supinated.

4.1. Ankle/Foot Kinematics

Since we incorporated the multi-segment OFM, we expected to see some differences in the magnitude of sagittal plane mobility at the ankle. For example, although the maximum dorsiflexion approximated 30 degrees, which was similar to Butler et al., Heredia et al. reported approximately 42 degrees [10,15]. The differences reported by Heredia et al. are likely related to the marker clusters and the simplified foot model used by that group. When the total sagittal plane motion of the forefoot, hindfoot, and talocrural joints is added together, Heredia et al.'s. findings were approximated [15]. This indicates that often overlooked intrinsic foot mobility is key to achieving full squat depth and should be considered clinically. Thus, it also becomes evident that using a multi-segment foot model was an advantage of our work and should be utilized in future studies [17]. Additionally, the use of the OFM allowed us to visualize previously unreported small, but important frontal plane abduction of the forefoot and transverse plane supination of the forefoot.

These motions are likely pivotal for optimal biomechanical proximal joint positioning. Being able to quantify the inter-foot mobility as part of the OHDS may be critical in the diagnosis, prognosis, and treatment planning for individuals who demonstrate functional impairments or low scores on the FMS^{TM}.

4.2. Knee Joint Kinematics

Sagittal and transverse plane motion during the squat followed a highly predictable pattern and demonstrated the least variability. The mean peak knee flexion of approximately 123 degrees was comparable to that reported by others [10,15]. However, our data did not distinguish subjects by FMS^{TM} score, whereas Butler and Heredia found that participants with FMS^{TM} scores of 1 and 2 demonstrated less peak flexion than those with an FMS^{TM} score of 3 [10,15]. These differences suggest that the FMS^{TM} score may be sensitive to inherent differences in how the squat is performed, as well as movement pathology. The mean tibiofemoral internal rotation, i.e., approximately 3.45°, peaked at 50% of the OHDS, a coupling pattern that has also been reported for walking and running activities [35–37]. This pattern is related to the "unlocking" of the knee during the initiation of the knee flexion and to the triplanar motion, dorsiflexion, eversion, and abduction of the foot [37]. Coupled tibiofemoral internal rotation and foot pronation is likely critical to the maintenance of the foot-flat position participants were instructed to hold. The large inter-individual variation, i.e., ranging from 9–12°, in knee axial rotation is likely related to the hierarchical nature of the calculation of Cardan angles [38]. Sex may also play a key role in this variability, and differences in the Q-angle should be considered when assessing in clinical settings [16]. The knee valgus peaked at larger knee flexion angles but was minimal and, like transverse plane angles, showed large inter-individual variation. The presence of high degrees of inter-individual variation casts doubt on the importance of frontal and transverse plane deviations when assessing clinically significant treatment strategies, as all research subjects were pain-free and without an injury history. However, the fidelity of transverse and frontal plane knee joint angles during the OHDS continues to be a goal of future research, as large movements in these planes have traditionally been associated with knee instability.

4.3. Hip Joint Kinematics

Participants initiated the squat slightly flexed (~11°) and reached a mean peak angle of approximately 120°. A mild hip flexion prior to beginning the squat is common and is likely related to prepositioning the trunk and pelvis, e.g., anterior pelvic tilt [39]. Our results were very similar to those reported by others, although, as noted for the knee, these previous studies reported changes in the peak hip flexion with differences in the FMS score [10,15]. As the hip flexed during the descent phase it abducted to a peak value of 19° abduction and 10° of internal rotation. As noted by others, coupled hip flexion and internal rotation are movement patterns found in both walking and running [35,36] and are likely related to joint and bony geometry, including acetabular position and femoral anteversion [23,37,40].

4.4. Trunk and Pelvic Segment Kinematics

With our biomechanical model, we determined trunk and pelvic segment movements relative to the laboratory coordinate system and the movement of the trunk relative to the pelvis. At squat initiation, the pelvis was preset at approximately 20° of anterior tilt, which is likely related to the forward lean of the trunk relative to the pelvis in order to control the body's center of mass (COM). During descent, the anterior pelvic tilt increased, likely related to increasing hip flexion, to approximately 33°. At the endpoint of the squat, there was a mild posterior pelvic tilt and backward trunk lean. This coupled movement likely occurred secondary to joint and soft tissue constraints in the lumbopelvic complex and served to maintain control of the COM. Squat ascent reversed this movement pattern with a return to a more anteriorly tilted pelvis and forward lean of the trunk. The relatively large

inter-individual variation in the trunk and pelvic segment kinematics was notable. This may be explained by the findings of List et al. that those with restricted tibial anterior translation altered the position of their trunk to maintain the center of mass and achieve maximal squat depth when compared to those who were able to advance the tibia more freely over the talocrural joint [13]. In healthy young participants, transverse and frontal plane movements of the trunk and pelvis were minimal, but the ability to measure these movements with some degree of fidelity may be critical for the documentation of pathomechanical movement patterns common to those with lumbago or unilateral pain or dysfunction.

4.5. Lower Extremity Kinetics

A net internal plantar flexor moment was present during both squat descent and ascent. It ranged from 0.20 Nm/Kg to its peak of approximately 0.28 Nm/kg during the descent phase. Peak plantarflexor moments in the current study were comparable to those reported by Butler et al. [10]. Since ankle power was absorbed (i.e., a mean of −0.10 W/kg) during squat descent, we conclude that the posterior tibial muscles were acting eccentrically to control tibial advancement. Conversely, power generation (i.e., a mean of approximately 0.10 W/kg) during the return phase suggests that the plantarflexors likely contributed to ankle stability and perhaps to knee extension. Frontal and transverse plane moments were small but present yet are relevant to provide stability as individuals were required to maintain their foot progression angle and a foot flat position.

Small net internal tibiofemoral flexor moments were noted at 0% (i.e., 0.14 Nm/kg) and 100% (i.e., 0.18 Nm/kg) of the OHDS, presumably to control knee extension prior to and following the squat. Knee flexion (during descent) and extension (during ascent) resulted in a peak net extensor moment of 0.85 Nm/kg. Butler et al. reported a range of mean peak knee extensor moments (from 0.45 Nm/kg to 0.63 Nm/kg) distinguished by the FMS score [10]. Since we did not distinguish joint motion or joint moments according to the FMS score, our data are not easily comparable to Butler et al. [10]. The knee moment differences may be related to differences in the sample demographics, biomechanical models, and segmental inertial properties used. During the descent phase, power was absorbed (i.e., mean peak of −1.3 W/kg) as the knee extensors were acting eccentrically, whereas during ascent, the knee extensors were acting concentrically and generating power (i.e., mean peak of 1.3 W/kg). Mean peak valgus (0.28 Nm/kg) and external rotator (0.30 Nm/kg) tibiofemoral moments, although small, may reflect the importance of both dynamic (muscular) and static (fascial and ligamentous) constraints during the OHDS. These data are unique to our report since previous research only documented sagittal plane knee moments.

As the hip flexed during squat descent, a mean peak net extensor moment of 0.76 Nm/kg was generated. This was associated with power absorption (−0.36 W/kg), confirming the eccentric action of the hip extensor muscles. Butler et al. reported a peak net hip extensor moment of 0.55 Nm/kg [10]. The substantial difference in hip extensor moments between Butler et al. and this report may also be related to differences in sample demographics, the biomechanical models, and the segmental inertial properties used [10,41]. After reaching the end range of the squat, the hip extensors acted concentrically, generating power (i.e., mean peak 0.50 W/kg). Small net hip adductor moments during squat descent (0.5 Nm/kg) were likely associated with eccentric action of the hip adductors that were used to control hip abduction and perhaps excessive frontal plane motion at the knee [42]. Similarly, small net hip external rotator muscle moments (i.e., mean peak of 0.15 Nm/kg) were generated to control hip internal rotation.

4.6. Limitations

One limitation of this study is that there were three separate sets of researchers who collected data, which could provide a source of error. However, all were trained by the PI, and good interrater reliability has been demonstrated for the PIG model [43]. Another limitation of this study is increased susceptibility to a transverse plane error caused by

the presence of only a single lateral thigh marker, as dictated by the PIG model, when a marker cluster on the thigh may have been superior when determining Cardan angle calculations for the frontal plane of the knee and transverse plane of both the knee and hip. This was in part controlled by the addition of medial femoral condyle and medial malleoli markers. Researchers posit that standard deviations for transverse plane data at the hip and tibiofemoral were often greater than those of other planes due to the biomechanical model that was used. Additionally, skin artifacts caused by the normal displacement of skin from the bony landmark during movement and occlusion of the ASIS marker at the deepest point of the squat are significant limitations when using adhesive markers for 3D motion analysis requiring mathematical algorithms and the use of Nexus Software to control. Moreover, these data were derived from a convenience sample of a young, healthy, population and may not be representative of a patient population or the population at large. Lower extremity skeletal abnormalities of the hip and knee were not screened for and may have contributed to the results. In future research, it may be important to screen for femoral version and varus/valgus alignment at the tibiofemoral joint.

Future research would benefit from more diverse sample populations with respect to age and injury history. It would also be beneficial for future research to address the correlation between OHDS performance differences and injury occurrence and explore gender differences and the differences in foot and ankle bony anatomy. Lastly, although Butler et al. and others address the correlation between FMS™ OHDS scores and kinematic, as well as kinetic, data, it would be beneficial for more specific data to be available on the foot and ankle [10].

5. Conclusions

Dynamic functional activities, such as the OHDS, are valuable for the assessment of functional movement and stability across multiple body segments and have become increasingly popular as methods of clinical assessment. 3D OHDS assessment likely provides a more comprehensive analysis than typically utilized 2-D assessments and allows for the consideration of multi-planar movements and interactions. These descriptive kinematic and kinetic data illustrate the involvement and interaction of sagittal, frontal, and transverse plane kinematics and kinetics during the OHDS. Although sagittal plane mobility is most visually apparent to clinicians due to the magnitude of movements occurring in this plane, the results of the current study yield valuable frontal and transverse plane data that could inform assessment and interventions related to the foot, knee, and hip. Due to this investigation's sample size and demographics, the collected data can serve as a pilot normative representation of OHDS performance for young and healthy adults.

Author Contributions: Conceptualization, B.J.H. and G.J.A.; methodology, B.J.H. and G.J.A.; formal analysis, B.J.H., G.JA., C.J.M., B.S.T. and L.A.G.; investigation, B.J.H., G.J.A., C.J.M., B.S.T. and L.A.G.; data curation, B.J.H., G.J.A., C.J.M., B.S.T. and L.A.G.; writing—original draft preparation, B.J.H., G.J.A., C.J.M., B.S.T. and L.A.G.; writing—review and editing, B.J.H., C.J.M. and G.J.A.; project administration, B.J.H. All authors have read and agreed to the published version of the manuscript.

Funding: This research received no external funding.

Institutional Review Board Statement: The study was conducted in accordance with the Declaration of Helsinki and approved by the Institutional Review Board of Grand Valley State University (14-026-H, approved 4 September 2018).

Informed Consent Statement: Informed consent was obtained from all subjects involved in the study.

Data Availability Statement: Not applicable.

Acknowledgments: The authors acknowledge Ryan Tisdall, Justin Victor, Christopher Wolbert, Justin VanDyke, Zachary Waugh, and Rhyan Wozniak who contributed to data collection.

Conflicts of Interest: The authors declare no conflict of interest.

References

1. Cuchna, J.W.; Hoch, M.C.; Hoch, J.M. The interrater and intrarater reliability of the functional movement screen: A systematic review with meta-analysis. *Phys. Ther. Sport* **2016**, *19*, 57–65. [CrossRef] [PubMed]
2. Dorrel, B.S.; Long, T.; Shaffer, S.; Myer, G.D. Evaluation of the Functional Movement Screen as an injury prediction tool among active adult populations: A systematic review and meta-analysis. *Sports Health* **2015**, *7*, 532–537. [CrossRef] [PubMed]
3. Garrison, M.; Westrick, R.; Johnson, M.R.; Benenson, J. Association between the functional movement screen and injury development in college athletes. *Int. J. Sports Phys. Ther.* **2015**, *10*, 21–28.
4. Schneiders, A.G.; Davidsson, A.; Hörman, E.; Sullivan, S.J. Functional movement screen normative values in a young, active population. *Int. J. Sports Phys. Ther.* **2011**, *6*, 75–82.
5. Teyhen, D.S.; Shaffer, S.W.; Lorenson, C.L.; Halfpap, J.P.; Donofry, D.F.; Walker, M.J.; Dugan, J.L.; Childs, J.D. The Functional Movement Screen: A reliability study. *J. Orthop. Sports Phys. Ther.* **2012**, *42*, 530–540. [CrossRef]
6. Clifton, D.R.; Grooms, D.R.; Onate, J.A. Overhead deep squat performance predicts Functional Movement Screen™ score. *Int. J. Sports Phys. Ther.* **2015**, *10*, 622–627.
7. Armstrong, R.; Greig, M. Injury identification: The efficacy of the functional movement screen™ in female and male rugby union players. *Int. J. Sports Phys. Ther.* **2018**, *13*, 605–617. [CrossRef]
8. Bonazza, N.A.; Smuin, D.; Onks, C.Y.; Silvis, M.L.; Dhawan, A. Reliability, validity, and injury predictive value of the Functional Movement Screen: A systematic review with meta-analysis. *Am. J. Sports Med.* **2016**, *45*, 725–732. [CrossRef]
9. Smith, C.A.; Chimera, N.J.; Wright, N.J.; Warren, M. Interrater and Intrarater Reliability of the Functional Movement Screen. *J. Strength Cond. Res.* **2013**, *27*, 982–987. [CrossRef]
10. Butler, R.J.; Plisky, P.J.; Southers, C.; Scoma, C.; Kiesel, K.B. Biomechanical analysis of the different classifications of the Functional Movement Screen deep squat test. *Sports Biomech.* **2010**, *9*, 270–279. [CrossRef]
11. Bell, D.R.; Oates, D.C.; Clark, M.A.; Padua, D.A. Two- and 3-dimensional knee valgus are reduced after an exercise intervention in young adults with demonstrable valgus during squatting. *J. Athl. Train.* **2013**, *48*, 442–449. [CrossRef]
12. Dill, K.E.; Begalle, R.L.; Frank, B.S.; Zinder, S.M.; Padua, D.A. Altered knee and ankle kinematics during squatting in those with limited weight-bearing–lunge ankle-dorsiflexion range of motion. *J. Athl. Train.* **2014**, *49*, 723–732. [CrossRef]
13. List, R.; Gülay, T.; Stoop, M.; Lorenzetti, S. Kinematics of the trunk and the lower extremities during restricted and unrestricted squats. *J. Strength Cond. Res.* **2013**, *27*, 1529–1538. [CrossRef]
14. Graci, V.; Van Dillen, L.R.; Salsich, G.B. Gender differences in trunk, pelvis and lower limb kinematics during a single leg squat. *Gait Posture* **2012**, *36*, 461–466. [CrossRef]
15. Heredia CLockie, R.G.; Lynn, S.K.; Paumukoff, D.N. Comparison of lower extremity kinematics during the overhead deep squat by Functional Movement Screen score. *J. Sports Sci. Med.* **2021**, *20*, 759–765. [CrossRef]
16. Mauntel, T.C.; Post, E.G.; Padua, D.A.; Bell, D.R. Sex Differences during an Overhead Squat Assessment. *J. Appl. Biomech.* **2015**, *31*, 244–249. [CrossRef]
17. Stebbins, J.; Harrington, M.; Thompson, N.; Zavatsky, A.; Theologis, T. Repeatability of a model for measuring multi-segment foot kinematics in children. *Gait Posture* **2006**, *23*, 401–410. [CrossRef]
18. Scattone Silva, R.; Maciel, C.D.; Serrão, F.V. The effects of forefoot varus on hip and knee kinematics during single-leg squat. *Man. Ther.* **2015**, *20*, 79–83. [CrossRef]
19. Han, D.; Nam, S.; Song, J.; Lee, W.; Kang, T. The effect of knee flexion angles and ground conditions on the muscle activation of the lower extremity in the squat position. *J. Phys. Ther. Sci.* **2017**, *29*, 1852–1855. [CrossRef]
20. Minick, K.I.; Kiesel, K.B.; Burton, L.; Taylor, A.; Plisky, P.; Butler, R.J. Interrater reliability of the Functional Movement Screen. *J. Strength Cond. Res.* **2010**, *24*, 479–486. [CrossRef]
21. Hollman, J.H.; Galardi, C.M.; Lin, I.-H.; Voth, B.C.; Whitmarsh, C.L. Frontal and transverse plane hip kinematics and gluteus maximus recruitment correlate with frontal plane knee kinematics during single-leg squat tests in women. *Clin. Biomech.* **2014**, *29*, 468–474. [CrossRef] [PubMed]
22. Roos, P.E.; Button, K.; van Deursen, R.W.M. Motor control strategies during double leg squat following anterior cruciate ligament rupture and reconstruction: An observational study. *J. NeuroEng. Rehabil.* **2014**, *11*, 19. [CrossRef] [PubMed]
23. Cook, G.; Burton, L.; Hoogenboom, B.J.; Voight, M. Functional movement screening: The use of fundamental movements as an assessment of function—Part 1. *Int. J. Sports Phys. Ther.* **2014**, *9*, 396–409.
24. Winter, D.A. *Biomechanics and Motor Control of Human Movement*, 4th ed.; John Wiley & Sons, Inc.: Hoboken, NJ, USA, 2009.
25. Woltring, H.J. A Fortran package for generalized, cross-validatory spline smoothing and differentiation. *Adv. Eng. Softw.* **1986**, *8*, 104–113. [CrossRef]
26. Balsdon, M.E.R.; Dombroski, C.E. Reliability of a multi-segment foot model in a neutral cushioning shoe during treadmill walking. *J. Foot Ankle Res.* **2018**, *1*, 60. [CrossRef]
27. Carson, M.C.; Harrington, M.E.; Thompson, N.; O'Connor, J.J.; Theologis, T.N. Kinematic analysis of a multi-segment foot model for research and clinical applications: A repeatability analysis. *J. Biomech.* **2001**, *34*, 1299–1307. [CrossRef]
28. Harrington, M.E.; Zavatsky, A.B.; Lawson, S.E.M.; Yuan, Z.; Theologis, T.N. Prediction of the hip joint centre in adults, children, and patients with cerebral palsy based on magnetic resonance imaging. *J. Biomech.* **2007**, *40*, 595–602. [CrossRef]
29. Murray, I.A.; Johnson, G.R. A study of the external forces and moments at the shoulder and elbow while performing every day tasks. *Clin. Biomech.* **2004**, *19*, 586–594. [CrossRef]

30. Parker, K.; Stebbins, J.; Bates, J. Comparing the Harrington and Davis method of hip joint centre localisation for unimpaired and pathological subjects. *Gait Posture* **2014**, *39*, S114–S115. [CrossRef]
31. Wright, C.J.; Arnold, B.L.; Coffey, T.G.; Pidcoe, P.E. Repeatability of the modified Oxford foot model during gait in healthy adults. *Gait Posture* **2011**, *33*, 108–112. [CrossRef]
32. Stief, F.; Böhm, H.; Michel, K.; Schwirtz, A.; Döderlein, L. Reliability and accuracy in three-dimensional gait analysis: A comparison of two lower body protocols. *J. Appl. Biomech.* **2013**, *29*, 105–111. [CrossRef]
33. Mantovani, G.; Ng, K.C.G.; Lamontagne, M. Regression models to predict hip joint centers in pathological hip population. *Gait Posture* **2016**, *44*, 48–54. [CrossRef]
34. Baker, R. *Measuring Walking: A Handbook of Clinical Gait Analysis*; Mac Keith Press: London, UK, 2013; Volume 56. Available online: http://doi.wiley.com/10.1111/dmcn.12288 (accessed on 24 June 2019).
35. DeLeo, A.T.; Dierks, T.A.; Ferber, R.; Davis, I.S. Lower extremity joint coupling during running: A current update. *Clin. Biomech.* **2004**, *19*, 983–991. [CrossRef]
36. Dierks, T.A.; Davis, I. Discrete and continuous joint coupling relationships in uninjured recreational runners. *Clin. Biomech.* **2007**, *22*, 581–591. [CrossRef]
37. Neumann, D.A. *Kinesiology of the Musculoskeletal System: Foundations for Rehabilitation*, 3rd ed.; Elsevier: St Louis, MO, USA, 2016.
38. Robertson, D.G.E.; Caldwell, G.E.; Hamill, F.; Kamen, G.; Whittlesey, S.N. *Research Methods in Biomechanics*, 2nd ed.; Human Kinetics: Boston, MA, USA, 2013.
39. Wing, A.; Flanagan, J.; Richardson, J. Anticipatory postural adjustments in stance and grip. *Exp. Brain Res.* **1997**, *116*, 122–130. [CrossRef]
40. Khamis, S.; Yizhar, Z. Effect of feet hyperpronation on pelvic alignment in a standing position. *Gait Posture* **2007**, *25*, 127–134. [CrossRef]
41. Kainz, H.; Carty, C.P.; Modenese, L.; Boyd, R.N.; Lloyd, D.G. Estimation of the hip joint centre in human motion analysis: A systematic review. *Clin. Biomech.* **2015**, *30*, 319–329. [CrossRef]
42. Cashman, G. The effect of weak hip abductors or external rotators on knee valgus kinematics in healthy subjects: A systematic review. *J. Sport Rehabil.* **2012**, *21*, 273–284. [CrossRef]
43. Schwartz, M.H.; Trost, J.P.; Wervey, R.A. Measurement and management of errors in quantitative gait data. *Gait Posture* **2004**, *20*, 196–203. [CrossRef]

Disclaimer/Publisher's Note: The statements, opinions and data contained in all publications are solely those of the individual author(s) and contributor(s) and not of MDPI and/or the editor(s). MDPI and/or the editor(s) disclaim responsibility for any injury to people or property resulting from any ideas, methods, instructions or products referred to in the content.